



HAL
open science

Impact of DOM source and character on the degradation of primidone by UV/chlorine: Reaction kinetics and disinfection by-product formation

Yuru Wang, Marie Couet, Leonardo Gutierrez, Sébastien Allard,
Jean-Philippe Croué

► To cite this version:

Yuru Wang, Marie Couet, Leonardo Gutierrez, Sébastien Allard, Jean-Philippe Croué. Impact of DOM source and character on the degradation of primidone by UV/chlorine: Reaction kinetics and disinfection by-product formation. *Water Research*, 2020, 172, pp.115463 -. 10.1016/j.watres.2019.115463 . hal-03489601

HAL Id: hal-03489601

<https://hal.science/hal-03489601>

Submitted on 7 Mar 2022

HAL is a multi-disciplinary open access archive for the deposit and dissemination of scientific research documents, whether they are published or not. The documents may come from teaching and research institutions in France or abroad, or from public or private research centers.

L'archive ouverte pluridisciplinaire **HAL**, est destinée au dépôt et à la diffusion de documents scientifiques de niveau recherche, publiés ou non, émanant des établissements d'enseignement et de recherche français ou étrangers, des laboratoires publics ou privés.



Distributed under a Creative Commons Attribution - NonCommercial 4.0 International License

1 **Impact of DOM source and character on the degradation of**
2 **primidone by UV/Chlorine: Reaction kinetics and disinfection**
3 **by-product formation**

4 Yuru Wang ^{a,c}, Marie Couet ^{b,c}, Leonardo Gutierrez ^{c,d}, Sébastien Allard ^c,
5 Jean-Philippe Croué ^{b,c} *

6
7 ^a Department of Environmental Science, School of Geography and Tourism, Shaanxi
8 Normal University, Xi'an 710119, China

9 ^b Institut de Chimie des Milieux et des Matériaux, IC2MP UMR 7285 CNRS,
10 Université de Poitiers, France

11 ^c Curtin Water Quality Research Centre, Department of Chemistry, Curtin University,
12 Australia

13 ^d Facultad del Mar y Medio Ambiente, Universidad del Pacifico, Ecuador

14
15
16
17 * Corresponding author: Tel: +33 (0) 7 87 09 44 66
18 E-mail address: jean.philippe.croue@univ-poitiers.fr

19
20
21

22 **Abstract:** The presence of Dissolved Organic Matter (DOM) can exert a strong
23 influence on the effectiveness of the UV/chlorine process. This study examined the
24 impact of five DOM isolates with different characteristics on the degradation kinetics
25 of model contaminant primidone (PM) during UV/chlorine treatment. The formation
26 of Disinfection By-Products (DBPs) from DOM after 15-min UV/chlorine treatment
27 followed by 24 h chlorination was investigated and compared with chlorination alone.
28 The use of chemical probes and radical scavengers revealed that $\cdot\text{OH}$ and $\text{ClO}\cdot$ were
29 the main radical species responsible for the loss of PM at acidic and alkaline
30 conditions, respectively. All tested DOM isolates significantly inhibited the decay of
31 PM. A strong negative correlation (>0.93) was observed between the decay rate
32 constants of PM and SUVA of DOM isolates, except for EfOM isolate, which induced
33 the strongest inhibitory effect due to its higher abundance in sulfur-containing
34 functional groups (i.e., sink of $\cdot\text{OH}/\text{Cl}\cdot$ radicals). Compared with chlorination, the
35 formation of Adsorbable Organic Chlorine (AOC) and Trichloromethane (TCM)
36 during the UV/Chlorine process was enhanced and hindered for low SUVA isolates
37 and high SUVA DOM, respectively. However, Dichloroacetonitrile (DCAN)
38 formation was generally lower for all isolates except for Ribou Reservoir DOM at pH
39 8.4 because of its high reactive nitrogenous DBP precursors at caustic conditions.
40 However, when normalized to the chlorine consumed, the UV/Chlorine process
41 always led to a lower DBPs formation compared with chlorination alone.

42

43 **Keywords:** UV/chlorine, Primidone, Dissolved Organic Matter, Disinfection

44 By-Products, SUVA

45

46

47 1. Introduction

48 Recently, the combination of UV irradiation and chlorine has gained increasing
49 scientific and technological interests as a promising Advanced Oxidation Process
50 (AOP) for drinking water, wastewater, and reclaimed water treatment. The UV
51 photolysis of chlorine generates hydroxyl radicals ($\cdot\text{OH}$) and chlorine radicals ($\text{Cl}\cdot$) as
52 the primary radical species which further react with HOCl/OCl^- and chloride ion,
53 leading to the formation of $\text{ClO}\cdot$ and $\text{Cl}_2\cdot^-$ as secondary radical species (Nowell and
54 Hoigné, 1992; Feng et al., 2007; Watts and Linden, 2007; Jin et al., 2011; Fang et al.,
55 2014; Chuang et al., 2017). It is well-known that $\cdot\text{OH}$ non-selectively oxidizes a
56 variety of substrates at nearly diffusion-controlled rates; which, however, could result
57 in a significant loss of efficiency in complex environmental matrices due to a radical
58 scavenging effect induced by background substances. Compared with $\cdot\text{OH}$, Reactive
59 Chlorine Species (RCS) are relatively less affected by solution chemistry, ascribing to
60 their more selective characteristics and preferentially targeting organic compounds
61 containing electron-rich moieties, such as phenols, anilines, olefins, and amines (Guo
62 et al., 2018; Zhang et al., 2019). Therefore, the diverse radical species simultaneously
63 present in the UV/chlorine process provide a higher efficiency toward a broader
64 spectrum of molecular structures and organic contaminants.

65 However, the radical chemistry of the UV/chlorine process is dependent on water
66 matrices. The pH affects the generation and transformation rates of radical species by
67 influencing the speciation of HOCl and OCl^- ($\text{pK}_a = 7.5$) (Watts and Linden, 2007).
68 Carbonates are known as important sinks of $\cdot\text{OH}$, $\text{Cl}\cdot$, and $\text{Cl}_2\cdot^-$ radicals ($k = 10^5 - 10^8$

69 $M^{-1} s^{-1}$), resulting in the formation of a relatively weak oxidizing carbonate radical
70 ($CO_3^{\cdot-}$) (Grebel et al., 2010; Zhang and Parker, 2018). Dissolved Organic Matter
71 (DOM, a highly heterogeneous mixture of organic molecules ubiquitously present in
72 aquatic environments) is of special concern because it exerts a strong influence on the
73 performance of the UV/chlorine process by playing multiple roles. The
74 light-absorbing chemical structures (i.e., chromophores) in DOM species can
75 attenuate the intensity of UV irradiation and consequently lead to a loss in photolytic
76 rate of chlorine decomposition; meanwhile, UV absorbed by DOM can generate
77 highly reactive species (e.g., $^3DOM^*$, 1O_2 , and $\cdot OH$) which will contribute to the
78 transformation of contaminants (Varanasi et al., 2018; Zhang and Parker, 2018).
79 Contrariwise, specific functional groups within DOM can induce significant
80 scavenging of radicals and consequently alter and complex the transformation of both
81 contaminants and DOM itself. The scavenging capacity of DOM depends on its
82 molecular composition and the specific reactivity of the existing organic moieties
83 with radical species. The apparent second-order rate constants for the reaction of
84 “generic” DOM with $\cdot OH$, $Cl\cdot$, and $ClO\cdot$ are 2.5×10^4 , 1.3×10^4 , and 4.5×10^4 $L\ mg^{-1}\ s^{-1}$,
85 respectively (Kong et al., 2018), suggesting that DOM is more susceptible to $ClO\cdot$
86 attack. Particularly, the importance of $ClO\cdot$ in the UV/chlorine process towards some
87 micropollutants has been recently highlighted due to its high concentration (i.e., 3-4
88 orders of magnitude higher than those of $\cdot OH$ and $Cl\cdot$) and relatively high reaction
89 rates ($k = 10^7 - 10^9\ M^{-1}\ s^{-1}$) (Guo et al., 2017). Nevertheless, the molecular diversity
90 of DOM can influence the overall radical reaction mechanism by promoting/inhibiting

91 preferential radical attack and, thus, significantly influence the efficiency of the
92 UV/chlorine process. Hence, exploring the influence of the origin and nature of
93 aquatic DOM on the underlying radical mechanisms controlled by the overall
94 scavenging effect is required to better understand the effectiveness of the UV/chlorine
95 process for removing specific contaminants.

96 In addition to altering substrate transformation kinetics and interacting with
97 photons, DOM incorporates major precursors of Disinfection By-Products (DBPs)
98 which are of serious human health and ecological concern during chlorination
99 processes. The quantities and speciation of DBPs formed are strongly affected by the
100 origin and character of the DOM (Kitis et al., 2002; Williams et al., 2019). Previous
101 studies demonstrated that the hydrophobic fraction of DOM rich in aromatic moieties
102 (e.g., phenolic structures and conjugated double bonds) contributes to a key pool of
103 DBPs precursors (Reckhow et al., 1990; Omby et al., 2018). The Specific UV
104 Absorbance at 254 nm (SUVA), i.e., used as a surrogate parameter to assess the
105 aromaticity and reactivity of DOM (Weishaar et al., 2003), generally correlates well
106 with the formation of regulated and unknown DBPs during chlorination (Croué et al.,
107 2000; Hua et al., 2015). The differential UV (i.e., change in UV absorbance of DOM)
108 was also observed as a good surrogate for DBP formation (Korshin et al., 1999;
109 Roccaro and Vagliasindi, 2009).

110 However, under UV/chlorine process conditions, DOM can be simultaneously
111 attacked by chlorine, the formed $\cdot\text{OH}$ radical, and RCS; thus, inducing the subsequent
112 modification of its reactivity towards chlorine and radical species (Li et al., 2016;

113 [Varanasi et al., 2018](#)). Therefore, the formation and distribution of DBPs in
114 UV/chlorine systems may significantly differ from those upon chlorination.
115 Nevertheless, the concern regarding the side effect of DBPs formation within the
116 UV/chlorine process is still debated, as previous studies have recorded contradictory
117 DBPs formations (i.e., probably due to significant differences in experimental setups)
118 ([Lamsal et al., 2011](#); [Li et al., 2016](#); [Wu et al., 2016](#); [Dong et al., 2017](#); [Wang et al.,](#)
119 [2017](#)). However, limited information is available regarding the role of DOM character
120 and associated correlation to DBPs formation in the UV/chlorine process.

121 The objective of this study was to investigate the impact of DOM source and
122 character on contaminant degradation kinetics by the UV/chlorine process and to
123 assess the formation of DBPs and Adsorbable Organic Chlorine (AOC). Five DOM
124 isolates of different origins (four surface waters and one treated urban wastewater)
125 and varying structural characteristics were examined. The changes in the properties of
126 DOM during the process were characterized by measuring the variation of the UV
127 absorption coefficient (cm^{-1}). Additionally, the radical chemistry under different
128 conditions for contaminant removal was elucidated. Primidone (PM), a typical
129 refractory micropollutant showing resistance to both UV photolysis and chlorination,
130 was selected as the model contaminant.

131 **2. Materials and method**

132 **2.1 Chemical reagents and DOM fractions**

133 Information on chemical reagents is provided in [Text S1](#) in the Supplementary
134 Information (SI). Five DOM fractions showing significant structural differences and

135 previously isolated from various sources were selected for this study: Hydrophobic
136 acids (i.e., DOM adsorbed onto XAD-8[®] resin at acid pH and recovered by caustic
137 desorption) extracted from Suwannee River water (S-HPOA, USA); hydrophobic
138 DOM fractions (i.e., similar protocol, however, eluted by the acetonitrile/water
139 desorption method) isolated from Ribou Reservoir (R-HPO, France), Black River
140 Reservoir (B-HPO, China), Colorado River (C-HPO, USA), and Jeddah Wastewater
141 (J-HPO, Saudi Arabia). The characteristics of the DOM isolates were summarized in
142 [Table 1](#).

143 **2.2 Experimental setup and procedures**

144 UV irradiation experiments were conducted with an LP-UV collimated beam
145 device ([Figure S1](#)) equipped with three 15 W low-pressure Hg UV-lamps ($\lambda = 254$ nm,
146 UV Technik Meyer, Germany) following the standard operation procedure suggested
147 by [Bolton and Linden \(2003\)](#). Reactions were performed using a glass petri dish
148 (inner diameter = 84 mm, volume = 200 mL) positioned on a mini magnetic stirrer to
149 provide a continuous mixing of the solution during the irradiation period. The average
150 UV irradiance across the solution reactor was determined as 0.835 mW cm^{-2} after
151 calibration and correction by a certified UVC radiometer (UV-surface, sglux,
152 Germany). The detailed information about the setup and the measurement of UV
153 irradiance are provided in [Text S2 \(SI\)](#).

154 For kinetic experiments, fluences of $50\text{-}750 \text{ mJ cm}^{-2}$ (i.e., $500\text{-}7500 \text{ J m}^{-2}$) were
155 applied to the prepared solutions unless otherwise indicated. Experiments were
156 conducted in solutions spiked with $5 \text{ }\mu\text{M}$ of primidone and 2.5 mM of phosphate

157 buffer (pH 5-9). Preliminary experiments showed that the 2.5 mM phosphate buffer
158 did not interfere with the degradation efficiency (data not shown). The reaction was
159 initiated by dosing a specific amount of free chlorine stock solution into the reactor
160 while simultaneously exposed to UV irradiation. Samples were collected at
161 predetermined time intervals and the residual chlorine was immediately quenched
162 with sodium metabisulphite in slight excess before analysis by High-Performance
163 Liquid Chromatography (HPLC) within 2 h. Experiments with UV alone and chlorine
164 alone under a free chlorine dose of 70 μM (i.e., 5 mg L^{-1}) in the dark were also
165 conducted to elucidate the role of UV photolysis and chlorination in contaminant
166 removal.

167 For DBPs formation tests, solutions of DOM isolate (5.0 mg-C L^{-1}) in 2.5 mM
168 phosphate buffer at pH 6.2 or 8.4 without contaminant addition were dosed with 70
169 μM free chlorine and were simultaneously subjected to UV irradiation for 15 min (UV
170 fluence = 340-550 mJ cm^{-2} depending on the DOM character). Subsequently, the
171 solutions were immediately transferred into amber bottles, sealed, and kept without
172 headspace for 24 h in the dark (i.e., chlorination). The chlorine residual was then
173 measured and quenched before analyzing trihalomethanes (THMs), haloacetonitriles
174 (HANs), and AOC1. For pre-UV experiments, the solutions were subjected to UV
175 irradiation for 15 min followed by the injection of 70 μM free chlorine for 24 hours.
176 The reaction was stopped with the addition of the reducing agent in slight excess. For
177 comparison purposes, DBPs formation from each DOM isolate by chlorination only
178 was examined using a similar approach without UV exposure. All experiments were

179 conducted at room temperature ($20\pm 2^\circ\text{C}$) in duplicate or triplicate, whereby the
180 average values were presented.

181 **2.3. Analytical methods**

182 *2.3.1 Analysis of residual PM, probes, and chlorine*

183 The concentrations of PM, nitrobenzene (NB), and benzoic acid (BA) were
184 quantified using an Agilent 1100 HPLC system equipped with an Agilent XDB C18
185 reversed-phase column (5 μm particle size, 250 mm \times 4.6 mm) and a Diode Array
186 Detector; while the wavelengths were set at 218, 270, and 230 nm for PM, NB, and
187 BA, respectively. The mobile phase was made of 50% methanol/50% phosphoric acid
188 (0.1%, V/V) and was eluted at a flow rate of 1.0 mL min^{-1} . The concentration of free
189 chlorine was determined using the DPD colorimetric method (Moore et al., 1984).

190 *2.3.2 Characterization of DOM isolates*

191 The specific UV absorbance (SUVA) for each DOM isolate was calculated as the
192 ratio of the UV absorption coefficient (cm^{-1}) at $\lambda = 254$ nm (Cary 60 UV-vis
193 spectrophotometer, Agilent, USA) to the concentration of Total Organic Carbon
194 (TOC) in solution (stock of ~ 5 mg-C L^{-1} of each isolate, Shimadzu TOC-L Analyzer,
195 Japan).

196 *2.3.3 THMs, HANs, and AOCl analysis*

197 THMs and HANs were analyzed by an Agilent 6890N GC interfaced with an
198 Agilent 5975 inert mass spectrometer and a headspace autosampler using a method
199 adapted from previously published analytic methods (Text S3). Samples for AOCl
200 analysis were enriched through adsorption on activated carbon column using a TOX

201 sample preparatory unit and then measured by combustion and ion chromatography
202 method using an Automatic Quick Furnace (AQF-100) with online Ion
203 Chromatography (Dionex ICS 3000) (Kristiana et al., 2015).

204 2.3.4 Kinetic Modeling

205 The UV/chlorine process was modeled using Kintecus V6.70 simulation software
206 to evaluate the steady-state concentrations of different radical species (Ianni, 2018).
207 Approximately 110 elementary reactions with rate constants obtained from the
208 literature were incorporated into the model (Fang et al., 2014; Guo et al., 2018). The
209 details of the principal reactions involved in this study are provided in Table S1.

210 3. Results and Discussion

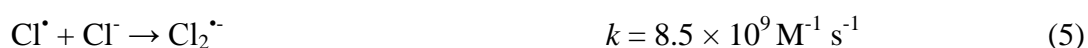
211 3.1 Kinetics of PM degradation

212 Preliminary experiments were conducted to investigate the loss of free chlorine (i.e.,
213 HOCl and OCl⁻) under UV photolysis at pH 5-9, and were reported in the SI section
214 (Text S4 and Figure S2). Initial experiments demonstrated that PM was
215 photo-resistant, resulting in a negligible removal (<4%) at the applied incident fluence
216 of 750 mJ cm⁻² across pH 5-9 (Figure S3). The degradation of PM under exposure to
217 70 μM free chlorine was also insignificant (<5%) due to the recalcitrance of amide
218 groups toward chlorination (Hureiki et al., 1994). In contrast, PM was efficiently
219 eliminated (>87%) in the UV/chlorine process because of the simultaneous generation
220 of [•]OH and RCS, as shown in Figure 1. The degradation of PM by the UV/H₂O₂
221 process was also investigated for comparison purposes. As shown in Figure 1, the
222 UV/chlorine AOP demonstrated a considerably higher efficacy for degrading PM.

223 Specifically the observed pseudo first-order rate constant (k_{obs} , $2.4 \times 10^{-4} \text{ s}^{-1}$) was 2.2
224 fold higher than that obtained from UV/H₂O₂ AOP ($1.1 \times 10^{-4} \text{ s}^{-1}$), likely attributed to
225 the reaction of PM with RCS as well as the higher quantum yields and molar
226 absorption coefficients of free chlorine species at 254 nm as compared with those of
227 H₂O₂. The quantum yields of HOCl, OCl⁻, and H₂O₂ under UV₂₅₄ were reported as
228 ~0.62-1.5, 0.55-1.3, and 0.5-1.1 mol Es⁻¹, respectively, while their molar absorption
229 coefficients were 59, 66, and 19.6 M⁻¹ cm⁻¹, respectively (Feng et al., 2007; Watts and
230 Linden, 2007; Jin et al., 2011; Fang et al., 2014; Sun et al., 2016; Chuang et al., 2017).

231 The initial dose of chlorine can affect the process efficiency by influencing the
232 speciation of radical species. The removal of PM significantly increased from 63% to
233 96% as chlorine dose increased from 10 to 50 μM. As a result, the corresponding k_{obs}
234 increased 2.7 fold (Figure 2a and b), suggesting a promoted radical exposure.
235 However, further increment in the chlorine dose to 100 μM resulted in minimal
236 enhancement of PM removal. The kinetic modeling indicated that under similar
237 conditions, the average ClO[•] content ranged from 10⁻¹⁰ to 10⁻⁹ M; specifically, 3~4
238 orders of magnitude higher than [•]OH content (Figure 2c). The modeled concentration
239 of Cl[•] was ~20% of the [•]OH concentration. Cl₂^{•-} was present at a considerably lower
240 level compared with other radicals. Both [•]OH and Cl[•] radicals gradually increased as
241 the chlorine dose increased from 10 to 50 μM, then leveled off due to the scavenging
242 effect of excess HOCl/OCl⁻ or Cl⁻ (i.e., present at ~equimolar of free chlorine
243 contributed from hypochlorite stock solutions); consequently, yielding more ClO[•] and
244 Cl₂^{•-} radicals (eqs. 1-5). As a result, the enhanced formation of the secondary ClO[•] and

245 $\text{Cl}_2^{\cdot-}$ radicals was calculated from the model with increasing chlorine concentration.
 246 However, the nonlinear increase in the rate constants of PM degradation suggests that
 247 the reactivity of ClO^{\cdot} with PM was not fast enough to offset the contributions of $\cdot\text{OH}$
 248 and Cl^{\cdot} scavenged by excess chlorine.



249 3.2 Contribution of different radical species

250 For differentiating the contribution of reactive radicals to PM decay in the
 251 UV/chlorine process, the $\cdot\text{OH}$ and Cl^{\cdot} concentrations were experimentally determined
 252 based on the degradation of NB and BA as relevant radical probes (Figure S4,
 253 calculation detailed in SI Text S5 and S6). Besides, the second-order rate constant of
 254 Cl^{\cdot} reaction with PM ($k_{\text{Cl}^{\cdot}, \text{PM}}$) was determined as $3.19 \times 10^{10} \text{ M}^{-1} \text{ s}^{-1}$ at pH 5 based on a
 255 similar approach and competition kinetics of PM and BA degradation in the
 256 UV/chlorine process. Under higher pH condition, the suspected contribution of ClO^{\cdot}
 257 led to a second-order rate constant higher than the diffusion-controlled rate constant.

258 Figure 3 illustrates the overall rate constants of NB, BA, and PM loss at pH 5-9 and
 259 the specific rate constants of PM degradation. Remarkably, the radical chemistry and
 260 the degradation of PM were not significantly affected by the presence of probes
 261 except for pH 5 (i.e., a condition that favors the production of $\cdot\text{OH}$ radicals) (Figure

262 S5). The performance of the UV/chlorine process was maximized at pH 5 with
263 complete removal of PM at 15 min. An increase in solution pH from 5 to 8.4 resulted
264 in a substantial decrease in the degradation rate of both probes and PM, while the rate
265 constants were not affected at alkaline conditions. Primidone (i.e., pK_a of ~ 12.3)
266 mainly occurred as one species and exhibited a similar photolysis rate under the
267 investigated pH range (Figure S3) (Schaffer et al., 2012). Thus, the significant pH
268 dependence of the UV/chlorine process efficiency in degrading PM was most likely
269 attributed to the shift in chlorine speciation toward OCl^- at increasing pH. The higher
270 abundance of OCl^- could enhance the scavenging of $\cdot OH$ and $Cl\cdot$ and simultaneously
271 increase the production of $ClO\cdot$ radical. As shown in Figure 3b, $\cdot OH$ was the main
272 radical species responsible for the loss of PM at acidic pH, while the degradation of
273 PM at alkaline conditions was mainly attributed to RCS species. At pH 7, both $\cdot OH$
274 and RCS participated in the PM decay under similar ratios ($\sim 42\%$ and 55% ,
275 respectively). As the solution pH increased from 5 to 9, $k_{\cdot OH}$ decreased from 3.5×10^{-3}
276 to $2.5 \times 10^{-4} s^{-1}$, while the contribution of $\cdot OH$ to the overall k_{obs} of PM loss decreased
277 from 88.8% to 14.7%. On the contrary, the corresponding contribution of RCS
278 increased from 9.4% to 82.5%.

279 To further distinguish the specific roles of individual RCS (i.e., $Cl\cdot$, $Cl_2\cdot^-$ and $ClO\cdot$)
280 on the degradation of PM, the impact of other radical promoter or scavenger was
281 investigated. The addition of 10 mM *tert*-butyl alcohol (TBA, a strong scavenger of
282 $\cdot OH$ and $Cl\cdot$) decreased the overall k_{obs} of PM degradation by 90% (from 4.29×10^{-3}
283 to $4.3 \times 10^{-4} s^{-1}$, Figure S6). TBA quenched $>99\%$ of $\cdot OH$, which contributed to 88.8%

284 of PM decay at pH 5. This finding suggested an insignificant involvement of Cl^\bullet for
285 PM transformation. The presence of 10 mM chloride had negligible effect on the
286 degradation rate of PM (Figure S7), although $\text{Cl}_2^{\bullet-}$ content increased by ~4 orders of
287 magnitude and the concentration of other radicals remained unchanged (Table S2).
288 This result supports the hypothesis that the role of $\text{Cl}_2^{\bullet-}$ radical was insignificant. The
289 presence of 100 mM HCO_3^- at pH 8.4 only resulted in a 1.7% and 7.6% decrease of
290 PM removal and decay rate, respectively (Figure S8). The kinetic modeling showed
291 that ~94% of OH^\bullet and Cl^\bullet were quenched by 100 mM HCO_3^- , whereas ClO^\bullet was not
292 affected due to its low reactivity toward HCO_3^- . Meanwhile, the model simulation
293 indicated that a relatively high concentration of $\text{CO}_3^{\bullet-}$ (5.37×10^{-10} M) was formed in
294 the system. Nevertheless, the contribution of $\text{CO}_3^{\bullet-}$ on the degradation of PM was
295 negligible because PM exhibited high resistance to $\text{CO}_3^{\bullet-}$ oxidation (Text S7 and
296 Figure S9). The above observations suggest that ClO^\bullet is the predominant reactive
297 radical responsible for the decay of PM at alkaline conditions. This result confirmed
298 the importance of ClO^\bullet in degrading some micropollutants, as previously reported
299 (Wu et al., 2016; Kong et al., 2018). TBA is a known efficient scavenger of both OH^\bullet
300 and Cl^\bullet ; however, its reactivity toward ClO^\bullet is still unclear. The second-order rate
301 constant for the reaction of TBA with ClO^\bullet was recently determined as $1.3 (\pm 0.1) \times$
302 $10^7 \text{ M}^{-1} \text{ s}^{-1}$ (Wu et al., 2017). However, our results showed that this value might be
303 highly overestimated given the minimal effect of 10 mM TBA on the degradation of
304 PM at pH 8.4 (Figure S8). Considering the predominant role of ClO^\bullet in PM
305 transformation at alkaline conditions, the second-order rate constant of ClO^\bullet with PM

306 was roughly estimated as $1.12 \times 10^6 \text{ M}^{-1} \text{ s}^{-1}$ at pH 8.4 by taking the specific k_{RCS} as
307 k_{ClO} and using its steady-state concentration from the model simulation. This value
308 was more than an order of magnitude lower than the one recently determined by Guo
309 et al. (2018) using competition kinetics. The reason for this difference is currently
310 unknown.

311 3.3 Impact of DOM character on the performance of the UV/chlorine process

312 In this study, the observed rate constants (Wu et al., 2017; Guo et al., 2018) were
313 used over the fluence-based rate constants (Miklos et al., 2019) to express the overall
314 reactivity of the processes because the UV irradiation absorbed by DOM also
315 generates highly reactive oxygen species (i.e., photosensitizer property) that can
316 contribute to the radical chemistry.

317 All 5 DOM isolates (5 mg-C L^{-1}) considerably inhibited the transformation of PM
318 in the UV/chlorine process; nevertheless, the degree of inhibition varied distinctively
319 depending on the character of the DOM isolate and the solution pH as shown in
320 Figure 4 and Figure S10. The rate constants for UV irradiation and chlorination only
321 were not plotted in the figures due to their negligible contribution to the degradation
322 of PM. The overall rate constants k_{obs} , specific rate constants k_{OH} , and k_{RCS} for PM
323 decay at pH 6.2 decreased by 54%-74%, 58%-82%, 44%-69%, respectively. The
324 addition of DOM at pH 8.4 induced a relatively slight decline in the process
325 performance compared with those at pH 6.2 with an 18%-37% and 19%-42%
326 decrease for k_{obs} and k_{RCS} , respectively. A strong negative correlation (>0.93) was
327 observed between the k_{obs} of PM degradation and SUVA except for J-HPO isolate. It is

328 well known that EfOM is enriched in organic sulfur (CHOS and CHNOS) originated
329 from detergents (Gonsior et al., 2011; Niu et al., 2018). S-containing functional
330 groups (e.g., sulfides) are preferentially susceptible to Cl^\bullet attack via single electron
331 transfer, donating electrons to C-H bonds, and resulting in enhanced H-abstraction by
332 $^\bullet\text{OH}/\text{Cl}^\bullet$ (Varanasi et al., 2018). Consequently, the J-HPO isolate (i.e., with a relatively
333 low SUVA but higher abundance in CHOS and CHNOS-compounds compared with
334 the four surface water DOM isolates) exhibited the strongest inhibitory effect on the
335 UV/chlorine process at pH 6.2 when $^\bullet\text{OH}$ and Cl^\bullet were relatively abundant in the
336 system. Except for the J-HPO isolate, the good correlation is consistent with the fact
337 that DOM isolates enriched with electron-rich moieties (e.g., conjugated double bond,
338 olefins, and amines) are more vulnerable to both $^\bullet\text{OH}$ and RCS attack (Wang et al.,
339 2017; Zhang and Parker, 2018). Compared with the control at pH 6.2, the presence of
340 S-HPOA DOM isolate (i.e., which showed the highest SUVA: 5.11) suppressed >70%
341 of both $^\bullet\text{OH}$ and Cl^\bullet based on the decay of probes; therefore, resulting in a 70%
342 decrease in k_{obs} of PM decay from 3.53×10^{-3} to $1.05 \times 10^{-3} \text{ s}^{-1}$, while the C-HPO
343 fraction (i.e., characterized by the lowest SUVA:1.92) exhibited the lowest inhibitory
344 effect. A good correlation could be established for k_{OH} at pH 6.2 and k_{RCS} at pH 8.4,
345 with SUVA. Nevertheless, k_{RCS} at pH 8.4 showed considerably higher linearity with
346 SUVA ($R^2 = 0.98$), suggesting that the aromatic components of DOM isolate are the
347 predominant sinks of ClO^\bullet . In contrast, other components (i.e., except for the
348 electron-rich groups) also contributed to the consumption of $^\bullet\text{OH}$. As elucidated by
349 Varanasi et al. (2018), $^\bullet\text{OH}$ can induce distinct transformation in the aliphatic

350 component of DOM. This may explain the significantly stronger inhibitory impact of
351 DOM at pH 6.2 than that of pH 8.4.

352 Since the UV absorbance of the DOM solution generally correlates well with the
353 activated aromatic moiety content, changes in UV_{254} during the UV/chlorine process
354 were recorded. The differential $UV_{254/15}$ absorbance ($\Delta UV_{254/15} = UV_{254, 0} - UV_{254, 15}$
355 $_{min}$), which refers to the cleavage of unsaturated C=C bonds of aromatic rings and
356 olefins, was calculated as a surrogate for DOM transformation. In agreement with
357 previous studies (Wang et al., 2017; Gao et al., 2019), UV/chlorine co-exposure
358 induced a more significant decrease in the UV absorbance of the DOM solutions;
359 while there was a minor decay by chlorine only and no significant decay by UV only.
360 The higher the initial SUVA, the larger the $\Delta UV_{254/15}$ (Figure S11). Strong correlations
361 could be established between $\Delta UV_{254/15}$ vs. $k_{\cdot OH}$ and k_{obs} at pH 6.2 or k_{RCS} and k_{obs} at
362 pH 8.4 (Figure 4), indicating that both $\cdot OH$ and $ClO\cdot$ play an important role in
363 degrading the conjugated structure of the chromophoric groups. Interestingly, the
364 relationship between $\Delta UV_{254/15}$ and $k_{\cdot OH}$ or k_{RCS} (established at pH 6.2 and pH 8.4,
365 respectively) fitted into the same linear correlation (Figure 4). This finding may
366 indicate that $\cdot OH$ and $ClO\cdot$ exert similar reactivity toward aromatic moieties.

367 3.4 DBPs formation from DOM isolates

368 Several series of experiments were conducted with five DOM fractions at pH 6.2
369 and pH 8.4 to compare the formation of DBPs upon chlorination only, UV followed
370 by chlorination, and combined UV/Chlorine process. AOC1, trichloromethane (TCM),

371 and dichloroacetonitrile (DCAN) were considered in the following discussion (i.e., no
372 noticeable amount of trichloroacetonitrile was detected in the chromatograms).

373 *3.4.1 Chlorination alone and Pre-UV chlorination*

374 The results obtained from chlorination experiments were in agreement with
375 previous findings (Hwang et al., 2001; Hua and Reckhow, 2008; Wang et al., 2015a).
376 For all fractions, the production of AOCl and DCAN was higher at pH 6.2 compared
377 with that at pH 8.4. Contrariwise, the formation of TCM was higher at pH 8.4 than at
378 pH 6.2. As previously observed (Wang et al., 2012), pre-UV irradiation led to the
379 decrease of TCM (i.e., no decrease with C-HPO) and DCAN production (Table S3);
380 however, no noticeable impact was observed for AOCl formation.

381 The formation of AOCl and TCM increased linearly with the SUVA of the DOM
382 fractions (Figure S12). For AOCl formation, a unique correlation for the two pH
383 conditions was obtained with the differential $UV_{254/24}$ absorbance values ($\Delta UV_{254/24} =$
384 $UV_{254,0} - UV_{254,24h}$); however, distinct correlations were observed for TCM (Figure 5).
385 Good exponential relationships were obtained between DCAN formation and C/N
386 ratio (Figure S13); the lower the C/N ratio, the higher the formation. R-HPO showed
387 the highest production of DCAN, a DOM fraction enriched in carboxyl-rich aliphatic
388 molecules (CRAM) incorporating nitrogen isolated from the Ribou Reservoir that is
389 known for being impacted by algal blooms (Niu et al., 2018).

390 *3.4.2 Combined UV/chlorine treatment*

391 UV/chlorine experiments were conducted using similar chlorination conditions as
392 the one used for chlorination alone (5 mg-C L⁻¹ of DOM, 70 μ M free chlorine). In the

393 presence of DOM, 50% to 90% of the injected chlorine was consumed after 15-min
394 irradiation (i.e., higher chlorine demand at pH 6.2 compared with pH 8.4), while only
395 15% was degraded in the absence of DOM (Figure S2 and S14). Overall, the higher
396 the SUVA, the higher the chlorine demand. A strong correlation was established
397 between the chlorine demand at 15 min and $\Delta UV_{254/15}$ (Figure 6). This correlation
398 excluded J-HPO which exerted a higher chlorine demand than expected from this
399 correlation.

400 No chlorine residual was recorded after 24 hours following 15-min UV/chlorine
401 treatment, except for C-HPO (lowest SUVA DOM), for which the chlorine residual
402 was 0.17 and 1.7 mg L⁻¹ at pH 6.2 and 8.4, respectively. As shown in Figure S11, the
403 chlorination reaction following the UV/chlorine co-exposure did not significantly
404 increase $\Delta UV_{254/15}$ (i.e., $\Delta UV_{254/24}$), which increased with SUVA and was higher at pH
405 6.2 than pH 8.4. However, the difference in $\Delta UV_{254/15}$ between UV/chlorine and
406 chlorine only was also observed with $\Delta UV_{254/24}$, especially for low and medium
407 SUVA DOM. This difference can be ascribed to the significant chlorine
408 consumption/degradation occurring during the UV/chlorine process, leading to the
409 production of radical species (i.e., more abundant at pH 6.2 than at pH 8.4) that are
410 highly reactive with aromatic moieties (Westerhoff et al., 1999; Varanasi et al., 2018).

411 The production of DBPs during chlorination and UV/chlorine processes is shown in
412 Figure S15. The ratios of the DBPs produced with the two processes were plotted as a
413 function of SUVA for comparing the results (Figure 7). At pH 6.2, good relationships
414 were obtained when excluding J-HPO from the data set; specifically, the lower the

415 SUVA, the higher the DBP ratios. The unique reactivity feature of J-HPO at pH 6.2
416 has been previously discussed; its higher sulfur-containing character enhanced its
417 reactivity with $\cdot\text{OH}/\text{Cl}$ by H-abstraction, which was apparently associated with the
418 degradation of DBP precursors. For low SUVA isolates C-HPO (1.92) and B-HPO
419 (2.45), the UV/Chlorine process enhanced AOC1 and TCM formation but decreased
420 DBP productions for high SUVA S-HPOA (5.11). At pH 6.2, moderate SUVA R-HPO
421 (3.24) showed no AOC1 and TCM difference between the two processes. At acid pH,
422 the AOP treatment showed lower DCAN formation for all isolates. At pH 8.4, good
423 relationships were also established when excluding the high THM and DCAN ratios
424 obtained for R-HPO, a fraction of DOM enriched in nitrogenous DBP precursors
425 originating from algal blooms (i.e., the base form of amino acids at pH 8.4 is more
426 reactive than the zwitterion form at pH 6.2). Except for DCAN results (i.e.,
427 comparable at both pH conditions), the difference between the two sets of data was
428 more significant at acid pH.

429 Similar findings have been discussed in the literature. [Li et al. \(2016\)](#) and [Wang](#)
430 [et al. \(2017\)](#) obtained a lower TCM formation with high SUVA DOM after
431 UV/chlorine exposure, compared with chlorine alone. [Wang et al. \(2015b\)](#) indicated
432 that the UV/chlorine process increased the DBP formation potential (FP) of low
433 SUVA treated water; the effect was generally more pronounced at pH 6.5 compared
434 with pH 8.5. However, contradictory results were also published showing an increase
435 ([Liu et al., 2012](#); [Sun et al., 2019](#)) or no modification ([Zhao et al., 2011](#)) of DBPFP
436 after the UV/chlorine treatment of high SUVA DOM. As previously discussed, pH

437 influences the distribution of radical species in solution and in particular controls the
438 abundance of $\cdot\text{OH}$ radical (i.e., more abundant at acid pH). The $\cdot\text{OH}$ radical may play
439 a major role in the transformation of organic matter during the UV/chlorine
440 co-exposure, which does not exclude the possible role of other radicals. The $\cdot\text{OH}$
441 radical can activate DBP precursors of low SUVA DOM, and degrade DBP precursors
442 of high SUVA DOM. In accordance with the current results, [Dotson et al. \(2010\)](#) and
443 [Metz et al. \(2011\)](#) observed an increase in TOX and/or TTHM formation after the
444 UV/H₂O₂ treatment of low SUVA treated river waters. This observation was attributed
445 to the reaction of $\cdot\text{OH}$ radical. Contrarywise, for a high SUVA river water (3.16),
446 [Lamsal et al. \(2011\)](#) observed a substantial decrease in TTHMFP. A decrease in
447 THMFP ([Sarathy and Mohseni, 2010](#)) and DCAN formation ([Chu et al., 2014](#); [Srithep
448 and Phattarapattamawong, 2017](#)) following UV/H₂O₂ treatment was also observed for
449 moderate (2.5-3.5) and low (1.3-1.9) SUVA waters.

450 If the current results are in good agreement with the literature, the experimental
451 conditions might have accentuated the difference between the chlorination and
452 UV/chlorine co-exposure results. Unlike the cited publications, only C-HPO showed
453 residual chlorine at the end of the reaction (24 hours). Results indicated that the
454 difference in DBPs formation from the two reaction conditions increased with the
455 amount of residual chlorine present after the 15-min UV/chlorine treatment ([Figure
456 S16](#)), suggesting that DBP formation from the UV/chlorine process could be
457 underestimated when compared with chlorine only. This finding does not compromise
458 our previous comments for low and moderate SUVA DOM isolates (C-HPO, B-HPO,

459 and R-HPO) and the effect of pH (i.e., no significant difference in chlorine demand
460 was observed at pH 6.2 and 8.4). For the high SUVA S-HPOA fraction, the significant
461 difference recorded between the two processes could be reduced with the use of a
462 higher chlorine dose allowing the presence of residual chlorine after 24 hours of
463 reaction. Because the chlorine dose applied for this study led to a major reduction of
464 the UV absorbing moieties (i.e., DBP precursors) during the 15-min UV/chlorine
465 treatment, the use of a higher chlorine dose should not significantly increase the TCM
466 formation. The unique reactivity of J-HPO should be further explored.

467 In [Figure 8](#), DBP formations were normalized to the chlorine consumed to take into
468 account the significant difference in chlorine demand between the two processes. As
469 observed by [Wang et al. \(2017\)](#) and for all DOM isolates and pH conditions, the
470 normalized (norm) DBP formation was always lower after UV/chlorine co-exposure
471 compared to chlorination and Pre-UV-Chlorination ([Figure S17](#)). Pre-UV irradiation
472 only slightly decreased norm-AOCl; more significant reductions were observed for
473 norm-TCM and norm-DCAN.

474 The relative abundances of TCM and DCAN to AOCl were depicted in [Figure S18](#).
475 At pH 6.2 and for all DOM isolates, TCM/AOCl ratios for the UV/chlorine process
476 were comparable or slightly higher in comparison with chlorination, while the
477 DCAN/AOCl ratios were significantly lower with the UV/chlorine process. At pH 8.4,
478 higher TCM/AOCl ratios were obtained for all DOM isolates with UV/chlorine
479 co-exposure (except for S-HPOA); nevertheless, DCAN/AOCl ratios remained lower
480 in the presence than in the absence of UV irradiation (except for R-HPO which

481 showed the opposite trend). However, the difference is less pronounced at pH 8.4.
482 These results indicate that radicals have diverse impacts on DBPs precursors. The
483 strong reactivity of nitrogenous organics with $\cdot\text{OH}$ radicals (Chu et al., 2014)
484 preferentially degrades DCAN precursors. $\cdot\text{OH}$ radicals seem to induce the formation
485 of TCM precursors while $\text{ClO}\cdot$, which is predominant at basic pH, may contribute to
486 TCM formation.

487 Finally, we should indicate that our lab-scale experimental conditions are truly
488 different from real field applications (i.e., irradiation time on the order of seconds
489 with much more powerful UV irradiance). Previous results obtained from full-scale
490 UV/chlorine trials suggested that RCS generated during the AOP process do not
491 significantly contribute to the formation of DBPs. It was proposed that the production
492 of $\cdot\text{OH}$ radicals during the UV/chlorine co-exposure, especially at lower pH, could
493 enhance the reactivity of DOM with chlorine due to the formation of stronger DBP
494 precursors susceptible to produce AOX and specific DBPs (i.e., HAN) at very short
495 contact time i.e., few seconds (Wang et al., 2015b; Wang et al., 2019).

496 **4. Conclusions**

497 In this study, the UV/chlorine process exhibited a significant synergetic effect in
498 eliminating PM (>87%) due to the simultaneous generation of $\cdot\text{OH}$ and RCS in the
499 system, while UV alone and chlorine only resulted in negligible PM decay. Modeling
500 and experimental results indicated that $\cdot\text{OH}$ is mainly responsible for the loss of PM at
501 acidic pH, while the degradation of PM at alkaline conditions was mainly attributed to
502 $\text{ClO}\cdot$. The presence of 5 mg-C L⁻¹ DOM substantially suppressed the k_{obs} of PM decay

503 in the UV/chlorine process by 18%-74%, depending on the DOM character and
504 solution pH. Except for J-HPO isolate, a strong negative correlation was observed
505 between the k_{obs} of PM degradation and the SUVA of DOM due to the high reactivity
506 of electron-rich moieties towards $\cdot\text{OH}$ and RCS attack. The J-HPO isolate, an EfOM
507 fraction with a relatively low SUVA but higher abundance in organic sulfur, exhibited
508 the strongest inhibition effect on the UV/chlorine process, likely resulting from the
509 enhanced sink of $\cdot\text{OH}$ and $\text{Cl}\cdot$ radicals by S-containing groups. Compared with
510 chlorination, the UV/chlorine process under our lab-scale experimental conditions
511 (i.e., UV/chlorine co-exposure during several minutes to reach the desired fluence;
512 conditions strictly different from few seconds contact time with much more intense
513 UV light that would be applied with full-scale treatment unit) promoted AOC1 and
514 TCM formation of low SUVA DOM but lowered the DBP productions for high SUVA
515 DOM. Nevertheless, the formation of DCAN was always lower during UV/chlorine
516 co-exposure, except for R-HPO, which exhibited higher production of DCAN at pH
517 8.4 due to its reactive form of nitrogenous DPB precursors at alkaline pH. Although
518 the irradiation conditions applied at lab-scale (i.e., longer contact time and much
519 lower UV intensity irradiance) are different from real applications, the observed
520 impact of DOM character (SUVA, a parameter commonly used by water treatment
521 plant operators to evaluate the chemical reactivity of DOM; S and N content) on the
522 degradation kinetics of contaminant and formation of DBPs from this study suggests
523 that DOM is an important parameter of the water matrix to control for optimizing the
524 operation of the UV/chlorine process.

525 Acknowledgments

526 The research reported in this study was supported by the National Natural Science
527 Foundation of China (No.51508317), the Fundamental Research Funds for the Central
528 Universities (GK201802108), China Postdoctoral Science Foundation
529 (No.2016M602762), and the Special Financial Grant from the Shaanxi Postdoctoral
530 Science Foundation (No.2017BSHTDZZ09). We gratefully acknowledge Professor
531 Xin Yang from Sun Yat-Sen University for the help about the kinetic modeling. The
532 valuable work of editor and anonymous reviewers is also appreciated.

533 Appendix A. Supplementary information

534 The supplementary information is found in a separate Microsoft Word document
535 (Supplementary Information section).

536

537 **References**

- 538 Bolton, J.R. and Linden, K.G., 2003. Standardization of methods for fluence (UV Dose) determination
539 in bench-scale UV experiments. *Journal of Environmental Engineering* 129(3), 209-215.
- 540 Chu, W., Gao, N., Yin, D., Krasner, S.W. and Mitch, W.A., 2014. Impact of UV/H₂O₂ Pre-Oxidation on
541 the Formation of Haloacetamides and Other Nitrogenous Disinfection Byproducts during
542 Chlorination. *Environmental Science & Technology* 48(20), 12190-12198.
- 543 Chuang, Y.-H., Chen, S., Chinn, C.J. and Mitch, W.A., 2017. Comparing the UV/Monochloramine and
544 UV/Free Chlorine Advanced Oxidation Processes (AOPs) to the UV/Hydrogen Peroxide AOP
545 Under Scenarios Relevant to Potable Reuse. *Environmental Science & Technology* 51(23),
546 13859-13868.
- 547 Croue', J.-P., Korshin, G.V. and Benjamin, M.M. 2000 Characterisation of Natural Organic Matter in
548 Drinking Water, AWWA Research Foundation, USA.
- 549 Dong, H., Qiang, Z., Hu, J. and Qu, J., 2017. Degradation of chloramphenicol by UV/chlorine
550 treatment: Kinetics, mechanism and enhanced formation of halonitromethanes. *Water Research*
551 121, 178-185.
- 552 Dotson, A.D., Keen, V.S., Metz, D. and Linden, K.G., 2010. UV/H₂O₂ treatment of drinking water
553 increases post-chlorination DBP formation. *Water Research* 44(12), 3703-3713.
- 554 Fang, J., Fu, Y. and Shang, C., 2014. The Roles of Reactive Species in Micropollutant Degradation in
555 the UV/Free Chlorine System. *Environmental Science & Technology* 48(3), 1859-1868.
- 556 Feng, Y., Smith, D.W. and Bolton, J.R., 2007. Photolysis of aqueous free chlorine species (HOCl and
557 OCl⁻) with 254 nm ultraviolet light. *J. Environ. Eng. Sci.* (6), 277-284.
- 558 Gao, Z.-C., Lin, Y.-L., Xu, B., Xia, Y., Hu, C.-Y., Zhang, T.-Y., Cao, T.-C., Chu, W.-H. and Gao, N.-Y.,
559 2019. Effect of UV wavelength on humic acid degradation and disinfection by-product formation
560 during the UV/chlorine process. *Water Research* 154, 199-209.
- 561 Gonsior, M., Zwartjes, M., Cooper, W.J., Song, W.H., Ishida, K.P., Tseng, L.Y., Jeung, M.K., Rosso, D.,
562 Hertkorn, N. and Schmitt-Kopplin, P., 2011. Molecular characterization of effluent organic matter
563 identified by ultrahigh resolution mass spectrometry. *Water Research* 45(9), 2943-2953.
- 564 Grebel, J.E., Pignatello, J.J. and Mitch, W.A., 2010. Effect of Halide Ions and Carbonates on Organic
565 Contaminant Degradation by Hydroxyl Radical-Based Advanced Oxidation Processes in Saline
566 Waters. *Environmental Science & Technology* 44(17), 6822-6828.
- 567 Guo, K., Wu, Z., Shang, C., Yao, B., Hou, S., Yang, X., Song, W. and Fang, J., 2017. Radical Chemistry
568 and Structural Relationships of PPCP Degradation by UV/Chlorine Treatment in Simulated
569 Drinking Water. *Environmental Science & Technology* 51(18), 10431-10439.
- 570 Guo, K., Wu, Z., Yan, S., Yao, B., Song, W., Hua, Z., Zhang, X., Kong, X., Li, X. and Fang, J., 2018.
571 Comparison of the UV/chlorine and UV/H₂O₂ processes in the degradation of PPCPs in simulated
572 drinking water and wastewater: Kinetics, radical mechanism and energy requirements. *Water*
573 *Research* 147, 184-194.
- 574 Hua, G. and Reckhow, D.A., 2008. DBP formation during chlorination and chloramination: Effect of
575 reaction time, pH, dosage, and temperature. *Journal American Water Works Association* 100(8),
576 82-+.
- 577 Hua, G., Reckhow, D.A. and Abusallout, I., 2015. Correlation between SUVA and DBP formation
578 during chlorination and chloramination of NOM fractions from different sources. *Chemosphere*
579 130, 82-89.

- 580 Hureiki, L., Croué, J.P. and Legube, B., 1994. Chlorination Studies of Free and Combined Amino
581 Acids. *Water Research* 28, 2521–2531.
- 582 Hwang, C.J., Krasner, S.W., Scilimenti, M.J., Amy, G.L., Dickenson, E., Bruchet, A., Prompsy, C.,
583 Giséle, F., Croue, J.-P., Violleau, D. and Leenheer, J. (2001) Polar NOM: Characterization, DBPs
584 and Treatment, American Water Works Association Research Foundation, Denver, CO, USA.
- 585 Ianni, J.C. 2018 Kintecus. Windows Version 6.70. <http://www.kintecus.com/>.
- 586 Jin, J., El-Din, M.G. and Bolton, J.R., 2011. Assessment of the UV/Chlorine process as an advanced
587 oxidation process. *Water Research* 45(4), 1890-1896.
- 588 Kitis, M., Karanfil, T., Wigton, A. and Kilduff, J.E., 2002. Probing reactivity of dissolved organic
589 matter for disinfection by-product formation using XAD-8 resin adsorption and ultrafiltration
590 fractionation. *Water Research* 36(15), 3834-3848.
- 591 Kong, X., Wu, Z., Ren, Z., Guo, K., Hou, S., Hua, Z., Li, X. and Fang, J., 2018. Degradation of lipid
592 regulators by the UV/chlorine process: Radical mechanisms, chlorine oxide radical (ClO center
593 dot)-mediated transformation pathways and toxicity changes. *Water Research* 137, 242-250.
- 594 Korshin, G.V., Kumke, M.U., Li, C.-W. and Frimmel, F.H., 1999. Influence of chlorination on
595 chromophores and fluorophores in humic substances. *Environmental Science & Technology* 33(8),
596 1207–1212.
- 597 Kristiana, I., McDonald, S., Tan, J., Joll, C. and Heitz, A., 2015. Analysis of halogen-specific TOX
598 revisited: Method improvement and application. *Talanta* 139, 104-110.
- 599 Lamsal, R., Walsh, M.E. and Gagnon, G.A., 2011. Comparison of advanced oxidation processes for the
600 removal of natural organic matter. *Water Research* 45(10), 3263-3269.
- 601 Li, T., Jiang, Y., An, X., Liu, H., Hu, C. and Qu, J., 2016. Transformation of humic acid and
602 halogenated byproduct formation in UV-chlorine processes. *Water Research* 102, 421-427.
- 603 Liu, W., Zhang, Z., Yang, X., Xu, Y. and Liang, Y., 2012. Effects of UV irradiation and UV/chlorine
604 co-exposure on natural organic matter in water. *Science of the Total Environment* 414, 576-584.
- 605 Metz, D.H., Meyer, M., Dotson, A., Beerendonk, E. and Dionysiou, D.D., 2011. The effect of
606 UV/H₂O₂ treatment on disinfection by-product formation potential under simulated distribution
607 system conditions. *Water Research* 45(13), 3969-3980.
- 608 Miklos, D.B., Wang, W.L., Linden, K.G., Drewes, E. and Huebner, U., 2019. Comparison of UV-AOPs
609 (UV/H₂O₂, UV/PDS and UV/Chlorine) for TOC removal from municipal wastewater effluent
610 and optical surrogate model evaluation. *Chemical Engineering Journal* 362, 537-547.
- 611 Moore, H.E., Garmendia, M.J. and Cooper, W.J., 1984. Kinetics of monochloramine oxidation of
612 N,N-diethyl-p-phenylenediamine. *Environmental Science & Technology* 18(5), 348-353.
- 613 Niu, X.-Z., Harir, M., Schmitt-Kopplin, P. and Croue, J.-P., 2018. Characterisation of dissolved
614 organic matter using Fourier-transformion cyclotron resonance mass spectrometry: Type-specific
615 unique signatures and implications for reactivity. *Science of the Total Environment* 644, 68-76.
- 616 Nowell, L.H. and Hoigné, J., 1992. Photolysis of aqueous chlorine at sunlight and ultraviolet
617 wavelengths—II. Hydroxyl radical production. *Water Research* 26(5), 599-605.
- 618 Onnby, L., Salhi, E., McKay, G., Rosario-Ortiz, F.L. and von Gunten, U., 2018. Ozone and chlorine
619 reactions with dissolved organic matter - Assessment of oxidant-reactive moieties by optical
620 measurements and the electron donating capacities. *Water Research* 144, 64-75.
- 621 Reckhow, D.A., Singer, P.C. and Malcolm, R.L., 1990. Chlorination of Humic Materials: Byproduct
622 Formation and Chemical Interpretations. *Environmental Science & Technology* 24, 1655-1664.

- 623 Roccaro, P. and Vagliasindi, F.G.A., 2009. Differential vs. absolute UV absorbance approaches in
624 studying NOM reactivity in DBPs formation: Comparison and applicability. *Water Research* 43(3),
625 744-750.
- 626 Sarathy, S. and Mohseni, M., 2010. Effects of UV/H₂O₂ advanced oxidation on chemical characteristics
627 and chlorine reactivity of surface water natural organic matter. *Water Research* 44(14), 4087-4096.
- 628 Schaffer, M., Boxberger, N., Boernick, H., Licha, T. and Worch, E., 2012. Sorption influenced transport
629 of ionizable pharmaceuticals onto a natural sandy aquifer sediment at different pH. *Chemosphere*
630 87(5), 513-520.
- 631 Srithep, S. and Phattarapattamawong, S., 2017. Kinetic removal of haloacetonitrile precursors by
632 photo-based advanced oxidation processes (UV/H₂O₂, UV/O₃, and UV/H₂O₂/O₃). *Chemosphere*
633 176, 25-31.
- 634 Sun, J., Kong, D., Aghdam, E., Fang, J., Wu, Q., Liu, J., Du, Y., Yang, X. and Shang, C., 2019. The
635 influence of the UV/chlorine advanced oxidation of natural organic matter for micropollutant
636 degradation on the formation of DBPs and toxicity during post-chlorination. *Chemical*
637 *Engineering Journal* 373, 870-879.
- 638 Sun, P., Lee, W.-N., Zhang, R. and Huang, C.-H., 2016. Degradation of DEET and Caffeine under
639 UV/Chlorine and Simulated Sunlight/Chlorine Conditions. *Environmental Science & Technology*
640 50(24), 13265-13273.
- 641 Varanasi, L., Coscarelli, E., Khaksari, M., Mazzoleni, L.R. and Minakata, D., 2018. Transformations of
642 dissolved organic matter induced by UV photolysis, Hydroxyl radicals, chlorine radicals, and
643 sulfate radicals in aqueous-phase UV-Based advanced oxidation processes. *Water Research* 135,
644 22-30.
- 645 Wang, C., Moore, N., Bircher, K., Andrews, S. and Hofmann, R., 2019. Full-scale comparison of
646 UV/H₂O₂ and UV/Cl₂ advanced oxidation: The degradation of micropollutant surrogates and the
647 formation of disinfection byproducts. *Water Research* 161, 448-458.
- 648 Wang, H., Zhu, Y., Hu, C. and Hu, X., 2015a. Treatment of NOM fractions of reservoir sediments:
649 Effect of UV and chlorination on formation of DBPs. *Separation and Purification Technology* 154,
650 228-235.
- 651 Wang, D., Bolton, J.R., Andrews, S.A. and Hofmann, R., 2015b. Formation of disinfection by-products
652 in the ultraviolet/chlorine advanced oxidation process. *Science of the Total Environment* 518,
653 49-57.
- 654 Wang, W.-L., Zhang, X., Wu, Q.-Y., Du, Y. and Hu, H.-Y., 2017. Degradation of natural organic matter
655 by UV/chlorine oxidation: Molecular decomposition, formation of oxidation byproducts and
656 cytotoxicity. *Water Research* 124, 251-258.
- 657 Wang, X., Hu, X., Wang, H. and Hu, C., 2012. Synergistic effect of the sequential use of UV irradiation
658 and chlorine to disinfect reclaimed water. *Water Research* 46(4), 1225-1232.
- 659 Watts, M.J. and Linden, K.G., 2007. Chlorine photolysis and subsequent OH radical production during
660 UV treatment of chlorinated water. *Water Research* 41(13), 2871-2878.
- 661 Weishaar, J.L., Aiken, G.R., Bergamaschi, B.A., Fram, M.S., Fujii, R. and Mopper, K., 2003.
662 Evaluation of specific ultraviolet absorbance as an indicator of the chemical composition and
663 reactivity of dissolved organic carbon. *Environmental Science & Technology* 37(20), 4702-4708.
- 664 Westerhoff, P., Aiken, G., Amy, G. and Debroux, J., 1999. Relationships between the structure of
665 natural organic matter and its reactivity towards molecular ozone and hydroxyl radicals. *Water*
666 *Research* 33(10), 2265-2276.

-
- 667 Williams, C.J., Conrad, D., Kothawala, D.N. and Baulch, H.M., 2019. Selective removal of dissolved
668 organic matter affects the production and speciation of disinfection byproducts. *Science of the*
669 *Total Environment* 652, 75-84.
- 670 Wu, Z., Fang, J., Xiang, Y., Shang, C., Li, X., Meng, F. and Yang, X., 2016. Roles of reactive chlorine
671 species in trimethoprim degradation in the UV/chlorine process: Kinetics and transformation
672 pathways. *Water Research* 104, 272-282.
- 673 Wu, Z., Guo, K., Fang, J., Yang, X., Xiao, H., Hou, S., Kong, X., Shang, C., Yang, X., Meng, F. and
674 Chen, L., 2017. Factors affecting the roles of reactive species in the degradation of
675 micropollutants by the UV/chlorine process. *Water Research* 126, 351-360.
- 676 Zhang, K. and Parker, K.M., 2018. Halogen Radical Oxidants in Natural and Engineered Aquatic
677 Systems. *Environmental Science & Technology* 52(17), 9579-9594.
- 678 Zhang, X., He, J., Xiao, S. and Yang, X., 2019. Elimination kinetics and detoxification mechanisms of
679 microcystin-LR during UV/Chlorine process. *Chemosphere* 214, 702-709.
- 680 Zhao, Q., Shang, C., Zhang, X., Ding, G. and Yang, X., 2011. Formation of halogenated organic
681 byproducts during medium-pressure UV and chlorine coexposure of model compounds, NOM and
682 bromide. *Water Research* 45(19), 6545-6554.

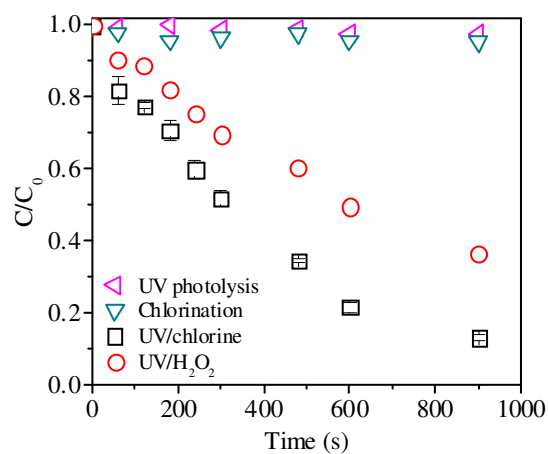


Figure 1. Degradation of PM by UV/chlorine and UV/H₂O₂ processes. Conditions: [PM] = 5 μ M, [free chlorine] = [H₂O₂] = 70 μ M, pH = 7.0.

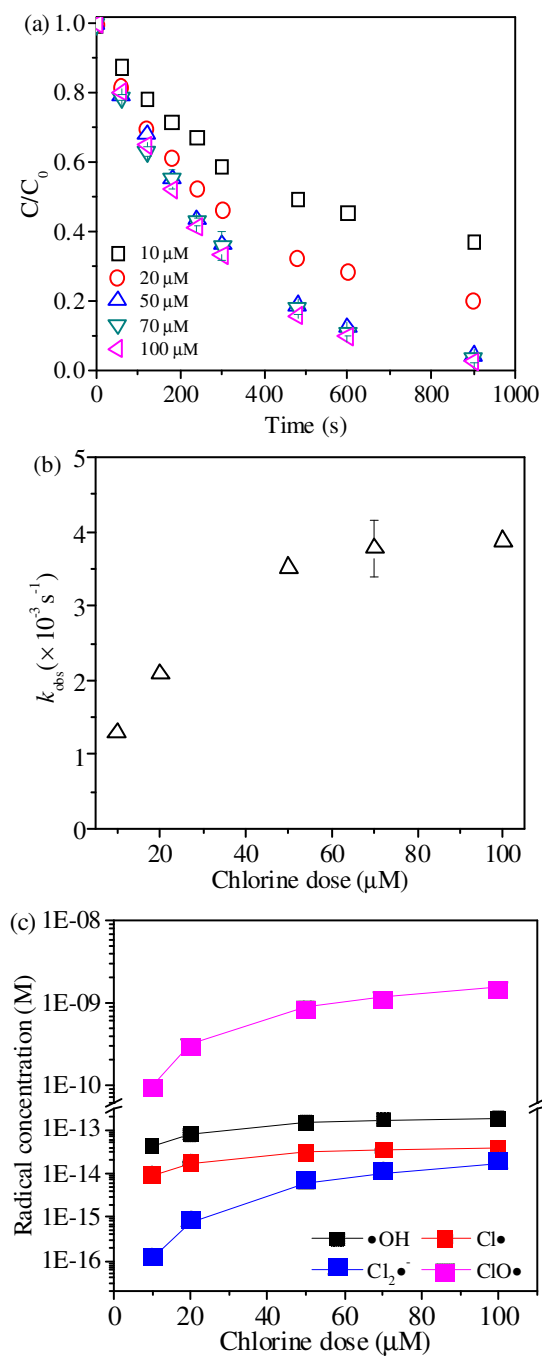


Figure 2. (a) Degradation of PM under different chlorine dose by the UV/Chlorine process, (b) the variation in the k_{obs} as a function of chlorine dose), and (c) average radical concentrations modelled for the first 10 min in the system. Conditions: $[\text{PM}] = 5 \mu\text{M}$, $\text{pH} = 6.2$.

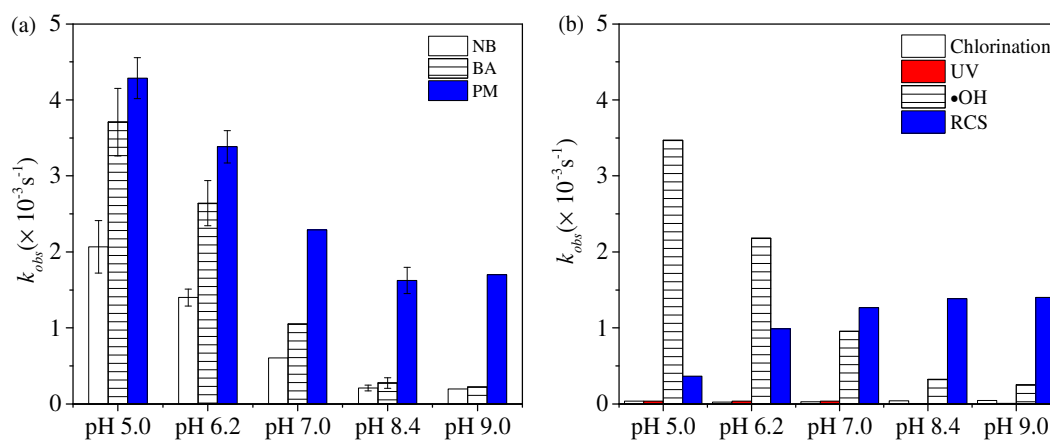


Figure 3. (a) Observed rate constants of the degradation of NB, BA, and PM under different pH by the UV/Chlorine process, and (b) Effect of pH on the specific rate constants of PM decay. Conditions: [free chlorine] = 70 μM , [PM] = 5 μM , [NB] = [BA] = 1 μM .

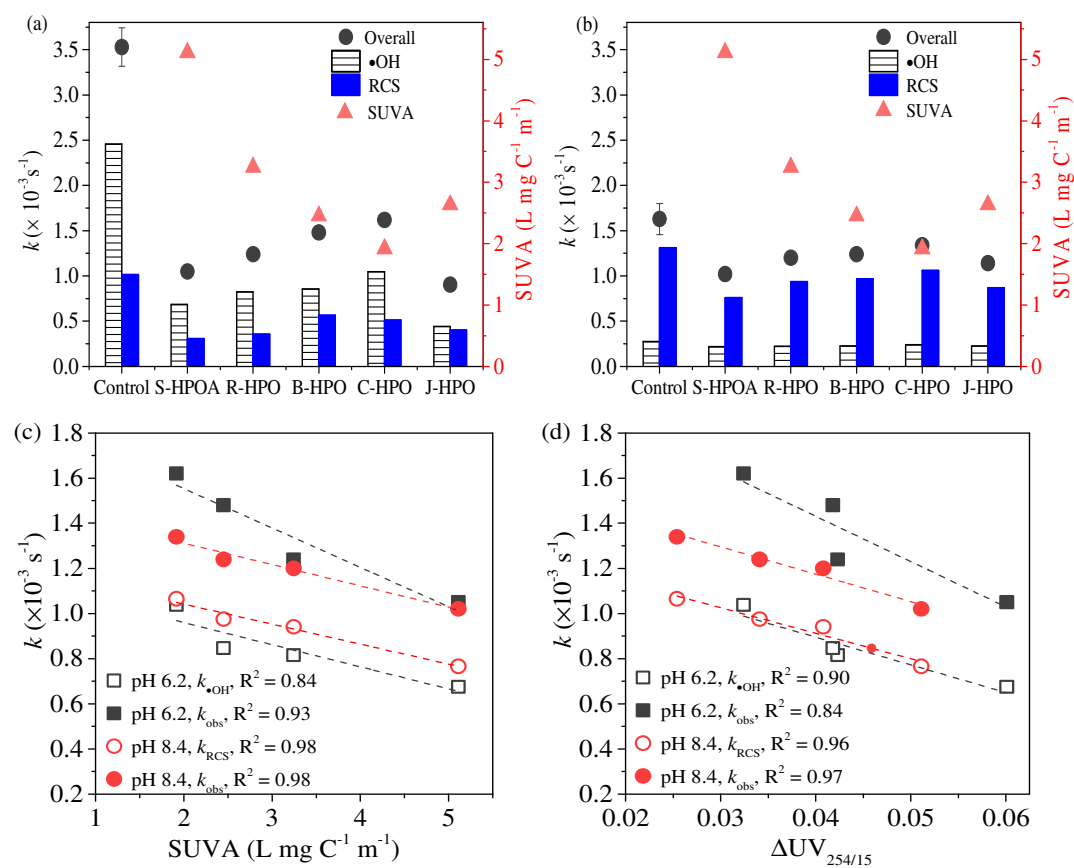


Figure 4. Effect of DOM isolates on the overall and specific rate constants of PM at pH 6.2 (a) and pH 8.4 (b) by the UV/Chlorine process, and correlations of the overall and specific rate constants of PM decay with the initial SUVA of the DOM isolates (c) and the $\Delta\text{UV}_{254/15}$ (d). Conditions: [free chlorine] = 70 μM , [PM] = 5 μM , [NB] = [BA] = 1 μM , 5 mg C L⁻¹ NOM.

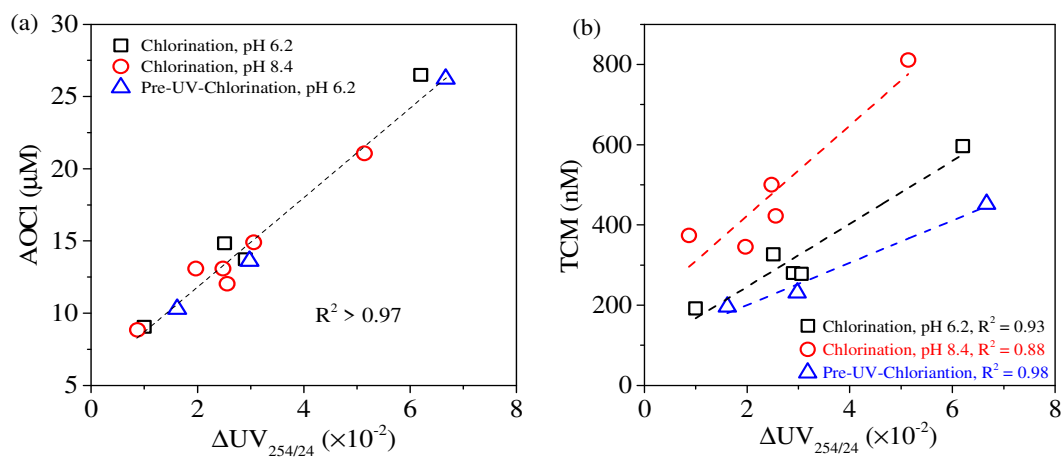


Figure 5. The formation of AOCI (a) and TCM (b) as a function of UV absorbance decay by chlorination and Pre-UV-Chlorination processes. Conditions: [free chlorine] = 70 μM , 5 mg-C L^{-1} DOM, using 2.5 mM phosphate buffer, 24 h of contact time.

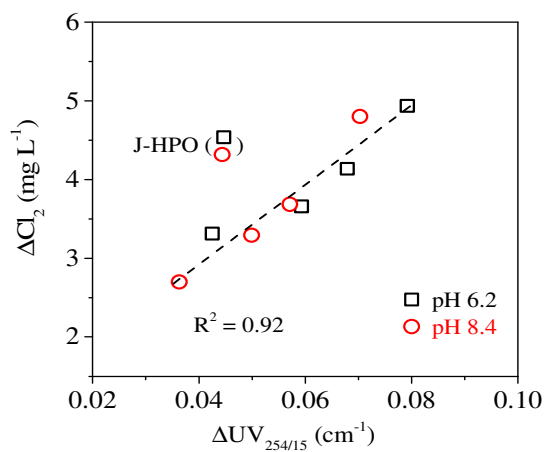


Figure 6. Relationship between the chlorine consumption and $\Delta\text{UV}_{254/15}$ during the 15-min UV/chlorine process for the 5 studied DOM isolates. Conditions: [free chlorine] = 70 μM , 5 mg-C L⁻¹ DOM, using 2.5 mM phosphate buffer.

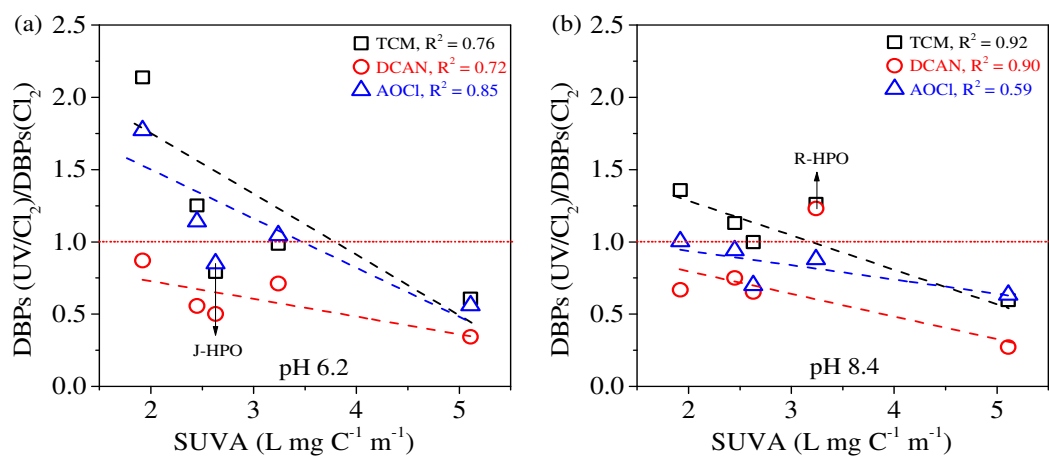


Figure 7. Ratios of the DBPs formation by the UV/chlorine process and chlorination as a function of the initial SUVA of DOM isolates at pH 6.2 (a) and pH 8.4 (b). Conditions: [free chlorine] = 70 μM , 5 mg-C L⁻¹ DOM, using 2.5 mM phosphate buffer, 24 h of contact time.

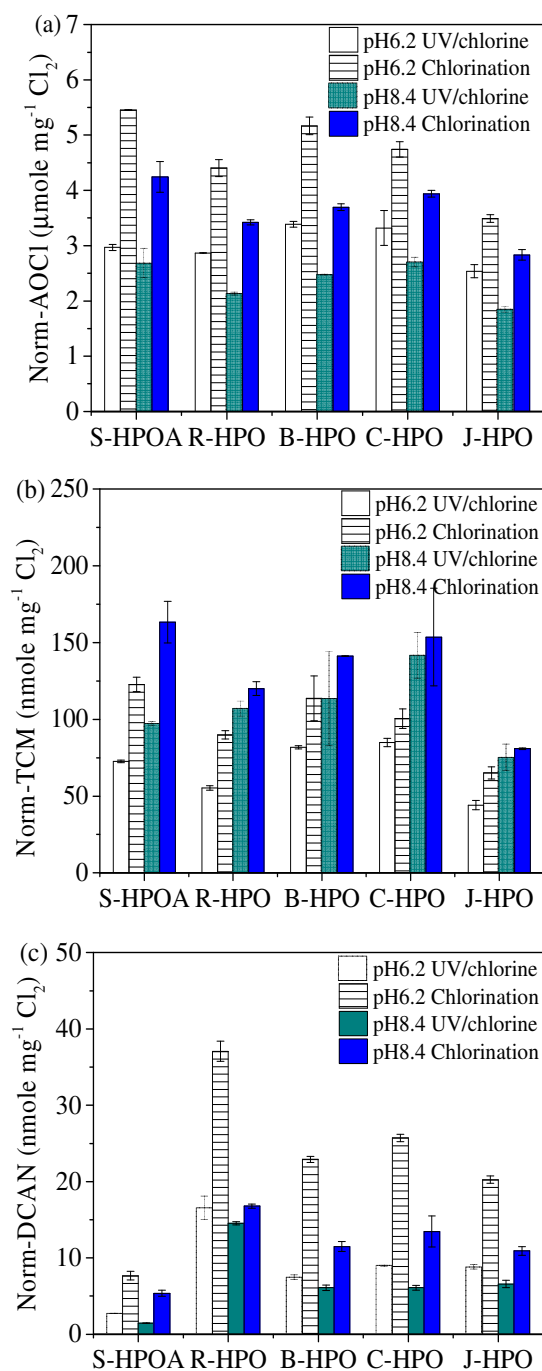


Figure 8. Comparison of norm-AOCl (a), norm-TCM (b), and norm-DCAN (c) formation from varying DOM isolates by UV/chlorine and Chlorination processes. Conditions: [free chlorine] = $70 \mu\text{M}$, 5 mg-C L^{-1} DOM, using 2.5 mM phosphate buffer, $I_0 = 0.835 \text{ mW/cm}^2$.

Table 1. Sources and Characteristics of NOM isolates

NOM source	Fraction ^a	Abbreviation	Mass ratio			SUVA ₂₅₄ ^b (L mg C ⁻¹ m ⁻¹)	Arom-C ^d %	DBE averag ^e	Ar ^e %
			C/H	C/N	C/O				
Suwannee River ^c	HPOA	S-HPOA	11.73	69.56	1.16	5.11	26.1	11.0	13.6
Ribou Reservoir ^d	HPO	R-HPO	9.53	18.41	1.27	3.24	16.0	9.9	6.7
Black River Reservoir	HPO	B-HPO	-	29.82	-	2.45	-	-	-
Colorado River ^d	HPO	C-HPO	9.10	35.2	1.40	1.92	13.2	9.6	2.5
Jeddah Wastewater ^c	HPO	J-HPO	8.98	19.51	2.13	2.63	24	7.0	9.7

^a HPOA: Hydrophobic acids; HPO: Hydrophobic.

^b SUVA₂₅₄: Specific ultraviolet absorbance was calculated from the absorption coefficient (cm⁻¹) at 254 nm (UV₂₅₄) divided by the corresponding DOC concentration (this study).

^c: (Croué et al., 2000)

^d: (Hwang et al., 2001).

^e: (Niu et al., 2018)

Graphical Abstract

